Synthesis of Surface-Initiated Stimuli-Responsive Diblock Copolymer Brushes Utilizing a Combination of ATRP and RAFT Polymerization Techniques

Misty D. Rowe, Brenton A. G. Hammer, and Stephen G. Boyes*

Department of Chemistry and Geochemistry, Colorado School of Mines, Golden, Colorado 80401

Received January 22, 2008; Revised Manuscript Received April 11, 2008

ABSTRACT: The synthesis of diblock copolymer brushes, including poly(styrene) (PSty)-*b*-PSty, PSty-*b*-poly(acrylic acid), PSty-*b*-poly(*N*-isopropylacrylamide), and poly(methyl acrylate)-*b*-poly(*N,N*-(dimethylamino)ethyl acrylate), was achieved utilizing a combination of surface-mediated atom transfer radical polymerization (ATRP) and reversible addition−fragmentation chain transfer (RAFT) polymerization techniques. Conversion of bromine end groups of homopolymer brushes formed by ATRP via a modified atom transfer addition reaction to a RAFT agent and diblock extension via RAFT polymerization allowed the direct formation of well-defined stimuli-responsive diblock copolymer brushes. The addition of sacrificial initiator and/or chain transfer agent permitted formation of well-defined diblock copolymer brushes and free polymer chains in solution. The free polymer chains were isolated and used to estimate the molecular weights and polydispersity index of chains attached to the surface. Ellipsometry, contact angle measurements, grazing angle attenuated total reflectance−Fourier transform infrared spectroscopy, and wide-scan X-ray photoelectron spectroscopy (XPS) were used to characterize initiator deposition, homopolymer brush formation via ATRP, conversion to macro-RAFT agent, and diblock copolymer brush formation via RAFT polymerization. Selective solvent treatment demonstrated the stimuli-responsive nature of the diblock copolymer brushes via changes in the water contact angles and wide-scan XPS atomic percentages.

Introduction

Living radical polymerization (LRP) techniques have the ability to provide simple and versatile routes for synthesizing polymers with well-defined molecular weight characteristics with both simple and complex architectures, due to minimal termination reactions resulting in polymer chains with "living" end groups. Atom transfer radical polymerization (ATRP) and reversible addition−fragmentation chain transfer (RAFT) polymerization are two of the most highly utilized LRP techniques because of their versatility in monomer, temperature, and solvent selection.[1–4] These fundamental characteristics of LRP techniques allow for the formation of well-defined surface-immobilized polymers via surface-initiated techniques, termed polymer brushes. Polymer brushes are typically characterized by high grafting densities resulting in uniform film thicknesses, and the use of LRP techniques also provides the ability to produce diblock copolymer architectures. ATRP and RAFT polymerization are arguably the most versatile LRP methods to prepare polymer-modified surfaces.[5–7] Historically, ATRP has been the most widely employed LRP technique for the formation of polymer brushes but has limitations in the synthesis of functional polymers, such as poly(acrylic acid) (PAA). Direct formation of well-defined PAA brushes has not thus far been achieved by ATRP due to the chelating capacity of the monomer to the metal catalyst which results in deactivation of the catalyst.[3] Typically, formation of PAA brushes by ATRP employs a postpolymerization modification step to deprotect the *tert*-butyl acrylate side groups by either acid hydrolysis or thermal cleavage to afford the acrylic acid functionality.[8–10]

Recently, RAFT polymerization has received a great deal of attention as a method to form polymer brushes due to its ability to polymerize highly functional monomers in a controlled fashion, and unlike ATRP, removal of a metal catalyst is not required.[6,11–14] While there have been a number of different methods reported for the immobilization of RAFT agents on various surfaces, one of the most promising techniques involves the conversion of immobilized ATRP initiators into RAFT agents.[6,11–17] One of the first examples of this technique was by Tsujii and co-workers, who converted surface-bound ATRP macroinitiators to terminal RAFT agent moieties, which allowed the utilization of both ATRP and RAFT polymerization techniques.[15] However, without the addition of Cu(0) to effectively shift the ATRP equilibrium to produce the activating species, Cu(I)Br, well-defined diblock copolymer brushes were not formed. Similarly, our group has recently produced well-defined diblock copolymer brushes by utilizing a modified atom transfer addition (ATA) reaction of surface-bound ATRP initiators to form surface-immobilized RAFT agents for the successful formation of well-defined diblock copolymer brushes.[6]

One of the primary goals in using LRP techniques to form polymer brushes is the production of "smart" surfaces.[8,18–20] These "smart" polymer films are produced by the formation of stimuli-responsive polymer brushes and have potential for application in a variety of different areas including controlled drug release, chromatographic separations, enhanced oil recovery, and optical switches.[5,7,9,10,20–23] Stimuli-responsive polymers undergo an abrupt change in property, such as conformation or solubility, when an external stimulus, such as solvent, temperature, or pH, is applied. Conformational changes brought about by stimulus change, such as change in solvent quality, when polymer chain ends are immobilized to surfaces is a well-documented example of a "smart" surface.[5,7,21,24] For example, Zhao et al. formed surface-immobilized stimuli-responsive diblock copolymer brushes via sequential cationic polymerization and ATRP.[21] By taking advantage of microphase separation of diblock copolymers due to solvent interaction parameters, they demonstrated the reversible solvent rearrangement capabilities of poly(styrene) (PSty)-*b*-poly(methyl methacrylate) (PMMA) and PSty-*b*-poly(methyl acrylate) (PMA) brushes.

Though stimuli-responsive polymer brush systems continue to gain interest, the ability to directly produce well-defined

* To whom correspondence should be sent: Ph (303) 273-3633; Fax (303) 273-3629; e-mail sboyes@mines.edu.

10.1021/ma800154c CCC: $40.75
Published on Web 05/30/2008

Scheme 1. General Route of Formation of Stimuli-Responsive, Diblock Copolymer Brushes through a Combination of Both Atom Transfer Radical Polymerization and Reversible Addition−Fragmentation Chain Transfer Polymerization Techniques

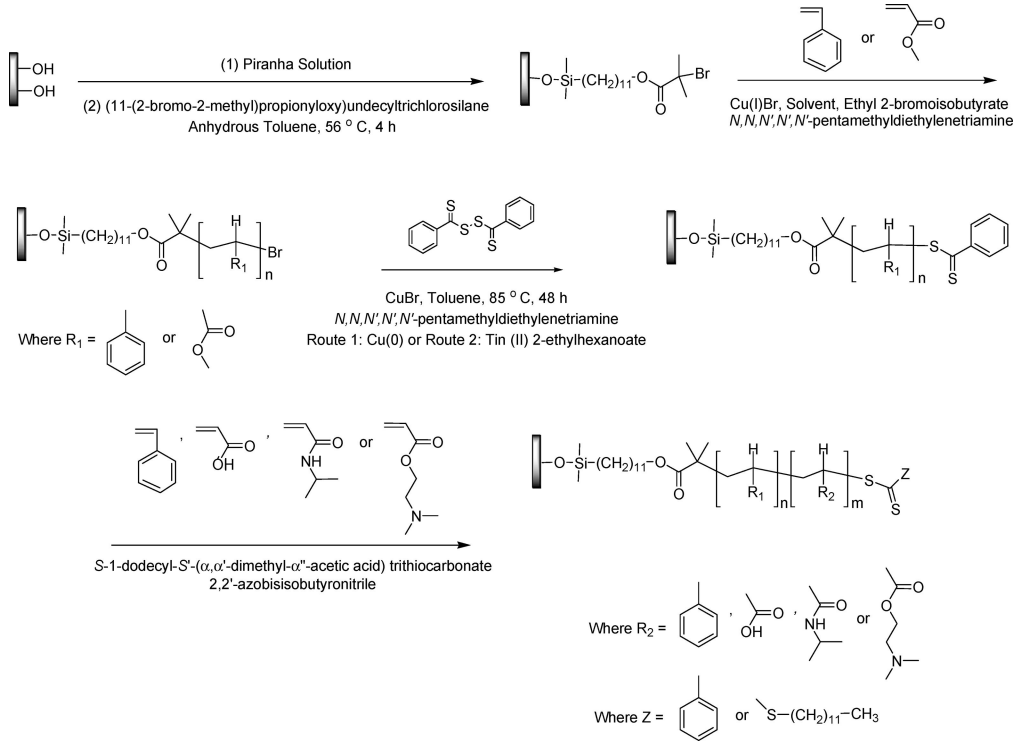

polymer brush systems of highly functional monomers has proven difficult. As such, this research will focus on providing a simple and versatile means of manipulating surface properties by producing "smart" polymer brushes utilizing a combination of both ATRP and RAFT polymerization techniques. By taking advantage of both ATRP and RAFT polymerization techniques, any available combination of monomers can be controllably polymerized in the formation of well-defined diblock copolymer brushes. To this effect, we have synthesized a variety of surface-initiated diblock copolymer brushes, including PSty-*b*-PAA, PSty-*b*-poly(*N*-isopropylacrylamide) (PNIPAM), and PMA-*b*-poly(*N*,*N*-(dimethylamino)ethyl acrylate) (PDMAEA), which have demonstrated reversible solvent switching capabilities. Formation of the inner block was achieved by immobilization of a typical ATRP initiator, (11-(2-bromo-2-methyl)propionyloxy)undecyltrichlorosilane (BMP TCS), and subsequent surface-initiated ATRP to produce PSty or PMA homopolymer brushes. For formation of the second block, these surface-immobilized ATRP macroinitiators were converted to a terminal RAFT agent moiety via an ATA reaction in a variation of a procedure previously reported by our research group.[6] Subsequent RAFT polymerization allowed for the direct formation of PAA, PNIPAM, and PDMAEA outer blocks. Ethyl 2-isobromobutyrate (E2-BiB) was added as a sacrificial initiator, in the polymerizations via ATRP, to control the surface polymerization and produce polymer in solution. Likewise, sacrificial RAFT agent, *S*-1-dodecyl-*S*′-(α,α′-dimethyl-α″-acetic acid) trithiocarbonate (DATC), was added to mediate synthesis of the outer blocks and form polymer in solution for the RAFT polymerizations. The general route for formation of surface-initiated, stimuli-responsive diblock copolymer brushes via the combination of ATRP and RAFT techniques is illustrated in Scheme 1.

Experimental Section

Materials. Copper (∼45 μm, powder, 99%), copper bromide (CuBr) (99%), anhydrous pyridine (99.0%), anhydrous tetrahydrofuran (THF) (stabilized with butylated hydroxytoluene, 99.9%), MA (stabilized with 10−20 ppm hydroquinone monomethyl ether (MEHQ), 99%), Sty (stabilized with 10−15 ppm *tert*-butylcatechol, 99%), AA (stabilized with 200 ppm MEHQ, 99.5%), and benzyl chloride (99%) were purchased from Acros Chemicals. Anhydrous methanol (HPLC grade), ethyl ether (certified ACS grade), potassium ferricyanide (reagent grade), and 30% hydrogen peroxide (certified ACS grade) were purchased from Fisher Scientific. NIPAM (97%), DMAEA (stabilized with 1000 ppm MEHQ, 98%), elemental sulfur (reagent grade, particle size ∼100 mesh), sodium methoxide (30 wt % solution in MeOH), *N,N,N′,N′,N′*-pentamethyldiethylenetriamine (99%) (PMDETA), E2-BiB (98%), 2,2′-azobisisobutrylnitrile (98%) (AIBN), tin(II) 2-ethylhexanoate (95%), anhydrous toluene (99.8%), ω-undecylenyl alcohol (98%), and 2-bromoisobutyryl bromide (98%) were purchased from Aldrich. Anhydrous *N,N*-dimethylformamide (DMF) (99.8%) was purchased from Acros. Trichlorosilane (98%) was obtained from Alfa Aesar. All other solvents were purchased from Mallinckrodt. Sty, MA, and DMAEA were passed through a basic alumina column and stored in the freezer prior to use. DMAEA and AA were distilled under pressure and stored in the freezer prior to use. NIPAM was recrystallized twice from hexanes before use. CuBr was purified via a literature procedure.[25] AIBN was recrystallized twice from methanol prior to use. Unless otherwise noted, all other chemicals were used as received. Silicon wafers were purchased from Wafer World, Inc., and cut into 2 × 6 cm pieces using a diamond-tipped glass cutter.

Synthesis of BMP TCS. BMP TCS was synthesized via a literature documented procedure.[26] ^{1}H NMR (400 MHz, $CDCl_3$, δ, ppm): 1.28−1.44 ($Cl_3Si(CH_2)_2(CH_2)_8$, br m, 16H), 1.59−1.68 ($Cl_3Si(CH_2)_2(CH_2)_8$, m, 4H), 1.78−1.81 ($C(CH_3)_2$, d, 6H), 4.08−4.19 ($-O(CH_2)CH_2$ m, 2H).

Synthesis of Dithiobenzoic Acid. Dithiobenzoic acid was synthesized following literature procedures.[27] Dithiobenzoic acid was not characterized as it degrades readily and was thus used immediately.

Synthesis of Dithiobenzoyl Disulfide (DTBDS). The synthesis of DTBDS was carried out according to a method in the literature.[27] ^{1}H NMR (400 MHz, $CDCl_3$, δ, ppm): 7.45 (dd, 4H, *m*-aromatic), 7.60 (m, 2H, *p*-aromatic), 8.07 (d, 4H, *o*-aromatic). ^{13}C NMR (100

MHz, $CDCl_3$, δ, ppm): 127.5 (*m*-aromatic), 128.0 (*o*-aromatic), 132.7 (*p*-aromatic), 219.0 (C═S). FTIR (cm^{-1}): 1021 (C═S), 3010 aromatic stretches.

Synthesis of DATC. DATC was prepared via Lai et al.'s literature procedure.[28] ^1H NMR (400 MHz, $CDCl_3$, δ, ppm): 0.89 ($S(CH_2)_{11}C\mathbf{H}_3$, t, 3H), 1.25−1.53 ($SCH_2(C\mathbf{H}_2)_{10}CH_3$, m, 20H), 1.73 ($SC\mathbf{H}_2(CH_2)_{11}CH_3$, s, 6H), 3.35 (t, 2H). FTIR (cm^{-1}): 1702 (C═O), 1065 (C═S).

Purification of Silicon Wafers. Silicon wafers were cleaned using a 30:70, v/v solution of 30% hydrogen peroxide and concentrated sulfuric acid. The solution was heated for 2 h at 100 °C. *Caution: piranha solution is extremely caustic.* Wafers were cleaned in deionized water, methanol, and methylene chloride sequentially, characterized, and used immediately for subsequent modification.

Deposition of BMP TCS. Previously cleaned wafers were placed in clean, dry glass tubes containing 25 mL of anhydrous toluene. 0.5 mL of 25 wt % solution of BMP TCS was added directly into the toluene by syringe, and the tubes were sealed. The reaction was heated to 56 °C for 4 h. Wafers were removed and sequentially cleaned with toluene, methanol, and methylene chloride and then dried in a stream of air.

Homopolymer Brush Formation via ATRP. The polymerization procedure to form PSty homopolymer brushes via ATRP involved the addition of Sty (13.5 mL, 1.17×10^{-1} mol), CuBr (5.50×10^{-2} g, 3.83×10^{-4} mol), and anhydrous anisole (16.5 mL) to a 150 mL Schlenk flask. The solution was degassed by bubbling high-purity nitrogen through the solution for 30 min and then left under a high-purity nitrogen atmosphere. The ligand PMDETA (0.157 mL, 8.19×10^{-4} mol) was added to the monomer solution and stirred until the solution became homogeneous. A wafer modified with BMP TCS was added to a second 150 mL Schlenk flask. The flask was sealed with a septum, subjected to three evacuation-high purity nitrogen purge cycles, and then left under a high-purity nitrogen atmosphere. The monomer solution was then transferred via cannula to the wafer containing flask, after which E2-BiB (46 μL, 3.1×10^{-4} mol) was added via syringe and the reaction was heated at 60 °C for 12 h (% conversion = 14%, $M_{n,theory}$ = 5735 g/mol, $M_{n,experiment}$ = 5240 g/mol, polydispersity index (PDI) = M_w/M_n = 1.05). Untethered polymer was removed from the wafers via Soxhlet extraction for 24 h in THF. Free polymer from the polymerization solution was isolated by evaporating residual monomer and solvent under vacuum overnight and purified by dissolving the polymer in THF and then passing the THF/polymer solution through a short column of activated basic alumina to remove any residual catalyst. The ATRP conditions per monomer for each of the other homopolymer brushes synthesized are as follows: Sty (13.5 mL, 1.17×10^{-1} mol), anhydrous anisole (16.5 mL), CuBr (5.50×10^{-2} g, 3.83×10^{-4} mol), PMDETA (0.157 mL, 8.19×10^{-4} mol), E2-BiB (46 μL, 3.1×10^{-4} mol), 60 °C, 24 h (% conversion = 28%, $M_{n,theory}$ = 11 468 g/mol, $M_{n,experiment}$ = 11 345 g/mol, PDI = 1.05) (% conversion = 20%, $M_{n,theory}$ = 8236 g/mol, $M_{n,experiment}$ = 8103 g/mol, PDI = 1.08). MA (10.0 mL, 1.1×10^{-1} mol), anhydrous anisole (20 mL), CuBr (5.50×10^{-2} g, 3.62×10^{-4} mol), PMDETA (0.15 mL, 3.6×10^{-4} mol), and E2-BiB (46 μL, 3.14×10^{-4} mol), 95 °C, 24 h (% conversion = 39%, $M_{n,theory}$ = 12 335 g/mol, $M_{n,experiment}$ = 13 963 g/mol, PDI = 1.21).

General Procedure for Modified ATA Reaction of Macro-ATRP Initiators. Anhydrous toluene (50 mL) and CuBr (0.150 g, 1.05×10^{-3} mol) were added to a 150 mL Schlenk flask equipped with a stir bar. The solution was degassed for 30 min by bubbling high-purity nitrogen through the solution in an ice bath and then left under a high-purity nitrogen atmosphere. Cu(0) (0.120 g, 1.87×10^{-3} mol) or tin 2-ethylhexanoate (1.53 mL, 1.87×10^{-3} mol), DTBDS (0.92 g, 1.36×10^{-3} mol), and wafers with PSty (ATRP) or PMA (ATRP) modified surfaces were added to a second 150 mL Schlenk flask. This flask was sealed with a septum, subjected to three evacuation−nitrogen purge cycles, and then left under a nitrogen atmosphere. PMDETA (1.20 mL, 6.25×10^{-3} mol) was added to the sealed CuBr containing flask and allowed to stir for 10 min to produce a homogeneous solution. The CuBr/PMDETA solution was transferred via cannula to the wafer containing flask. Finally, E2-BiB (0.060 mL, 4.08×10^{-6} mol) was added to the combined solutions via syringe, and the reaction was allowed to heat at 85 °C for 48 h. After this time, the wafers were removed and cleaned sequentially with toluene, methanol, and methylene chloride. Additionally, residual copper was removed via Soxhlet in THF for 24 h before characterization by ellipsometry and goniometry.

Diblock Copolymer Brush Formation via RAFT Polymerization. An example polymerization procedure to form diblock copolymer brushes via RAFT polymerization involved the addition of Sty (50 mL, 0.434 mol), AIBN (0.157 g, 9.56×10^{-4} mol), and DATC (1.64 g, 4.50×10^{-3} mol) to a 150 mL Schlenk flask. The solution was degassed for 30 min by bubbling high-purity nitrogen through the solution in an ice bath and was then left under a high-purity nitrogen atmosphere. A wafer with PSty (ATRP) modified by ATA reactions was added to a second 150 mL Schlenk flask. The flask was sealed with a septum, subjected to three evacuation−purge cycles, and then left under a high-purity nitrogen atmosphere. The monomer solution was then transferred via cannula to the wafer-containing flask, and the reaction was heated at 90 °C for 12 h (% conversion = 54%, $M_{n,theory}$ = 5468 g/mol, $M_{n,experiment}$ = 5342 g/mol, PDI = 1.11). Untethered polymer was removed from the wafers via Soxhlet extraction for 24 h in THF. Free polymer from the polymerization solution was isolated by evaporating residual monomer and solvent under vacuum overnight. The RAFT polymerization conditions per monomer for each of the other outer blocks for the diblock copolymer brushes synthesized are as follows: Sty (50 mL, 0.434 mol), AIBN (0.157 g, 9.56×10^{-4} mol), and DATC (1.64 g, 4.50×10^{-3} mol) at 90 °C for 12 h (% conversion = 42%, $M_{n,theory}$ = 4395 g/mol, $M_{n,experiment}$ = 4657 g/mol, PDI = 1.08). AA (20 mL, 0.294 mol), DMF (45.5 mL), DATC (0.7620 g, 2.10×10^{-3} mol), AIBN (0.0343 g, 2.10×10^{-4} mol), 60 °C, 24 h (% conversion = 94%, $M_{n,theory}$ = 14 335 g/mol, $M_{n,experiment}$ = 10 888 g/mol, PDI = 1.10). NIPAM (6.53 g, 5.77×10^{-2} mol), DMF (25 mL), DATC (0.269 g, 7.38×10^{-4} mol), AIBN (2.90×10^{-2} g, 1.77×10^{-4} mol), 60 °C, 18 h (% conversion = 96%, $M_{n,theory}$ = 8733 g/mol, $M_{n,experiment}$ = 8606 g/mol, PDI = 1.12). DMAEA (10 mL, 6.50×10^{-1} mol), anhydrous toluene (12 mL), DATC (1.50×10^{-1} g, 4.12×10^{-4} mol), AIBN (3.6×10^{-3} g, 5.50×10^{-5} mol), 60 °C, 12 h (% conversion = 76%, $M_{n,theory}$ = 17 451 g/mol, $M_{n,experiment}$ = 15 120 g/mol, PDI = 1.25).

Solvent Treatment of Diblock Surfaces. PSty-*b*-PAA, PSty-*b*-PNIPAM, and PMA-*b*-PDMAEA polymer brushes were subjected to different solvents to monitor their rearrangement properties. The surfaces were first exposed to a solvent that is good for both blocks in order to fully extend the diblock and to position the outer block at the air−polymer interface. Second, the surfaces were exposed to a solvent that is a poor solvent for the outer polymer layer, but a good solvent for the inner polymer layer, to stimulate rearrangement of the diblock copolymer−polymer brush by forcing the outer block away from the air interface, while bringing the inner block to the air interface.

For the PSty-*b*-PAA and PSty-*b*-PNIPAM diblock copolymer surfaces, wafers were immersed in anhydrous DMF (15 mL), a solvent that is good for both polymer blocks, in dried deposition tubes. For the PMA-*b*-PDMAEA diblock copolymer surface, the wafer was immersed in anhydrous toluene (15 mL), a solvent that is good for both polymer blocks, in a dried deposition tube. In each case, the deposition tubes were heated at 40 °C for 1 h to facilitate extension of the diblock copolymer brushes. The diblock copolymer brushes were then subjected to a poor solvent for the outer polymer blocks, but a good solvent for the inner blocks, in dry deposition tubes. In the case of the PSty-*b*-PAA and PSty-*b*-PNIPAM samples the solvent was cyclohexane, and for the PMA-*b*-PDMAEA sample the solvent was dichloromethane. The deposition tubes were heated at 40 °C for 1 h to facilitate rearrangement of the outer block. Wafers were dried via a stream of nitrogen then characterized immediately by goniometry and XPS.

Characterization. Ellipsometric measurements were carried out on a Gaertner ellipsometer, model L116C, with a 632.8 nm helium−neon laser at a 70° angle of incidence. Refractive indices were fixed at 1.455 for all respective surface modifications and brushes. Contact angle measurements were performed utilizing a Rame-Hart goniometer with a 10.0 μL syringe. Static (θ_s), advancing (θ_a), and receding (θ_r) water contact angles were recorded at 0° and 35°. Five measurements were taken across each sample, with their average being used for analysis. Grazing angle attenuated total reflectance (GATR)−Fourier transform infrared (FTIR) spectra were collected utilizing a Harrick Scientific GATR-FTIR attachment coupled with a Thermo-Electron Nicolet 4700 spectrometer, collecting 256 sample scans, and utilizing Nicolet's OMNIC software. All nuclear magnetic resonance (NMR) spectra (^{1}H NMR 400 MHz; ^{13}C NMR 100 MHz) were obtained from a Varian Gemini spectrometer using the MestReC software package. All samples were collected at 25 °C in deuterated chloroform ($CDCl_3$), with the exception of the poly(acrylic acid), which was collected in deuterated *N,N*-dimethyl sulfoxide. Molecular weight analysis was performed utilizing gel permeation chromatography (GPC) with THF or DMF as the eluent. The system was comprised of a Viscotek 270max system with three ViscoGel columns with a linear range of molecular weights from 20K to 10M g/mol connected in series. The THF GPC was a triple detector system comprised of an Eldex column heater (model CH-150 (30 °C)), a Viscotek differential viscometer/low-angle laser light scattering detector (model 270, λ = 670 nm, 3 mW laser, detector angles of 7° and 90°), a UV/vis detector (model 3210, λ = 254 nm, tungsten/deuterium lamp), and a refractive index detector (model 3580 (10 mV, λ = 660 nm)). ChromAR grade THF was used as eluent at a flow rate of 1.0 mL/min. All polymer samples were dissolved in ChromAR grade THF (5 mg/mL) and were injected using a variable injection volume autosampler. The refractive index increment (d*n*/d*c*) for PSty and PMA were 0.185 and 0.056 mL/g, respectively.[29] Molecular weight data analysis collected in THF was performed using Viscotek OmniSEC software. Similarly, GPC employing DMF (0.02 M LiBr) as the eluent utilized the same Viscotek components with two ViscoGel I-Series mixed bed columns, G-3000 and G-4000, and samples were run at 60 °C. PNIPAM samples were dissolved in chromatography grade DMF (5 mg/mL) utilizing a d*n*/d*c* value of 0.077 mL/g, which was calculated by the instrument. Both organic GPCs were standardized using PSty (98 000 and 250 000 g/mol) and PMMA (75 000 and 150 000 g/mol) standards. Aqueous GPC was employed using SynChropak CATSEC columns (100, 300, and 1000 Å; Eichrom Technologies Inc.) and 1 wt % acetic acid/0.1 M Na_2SO_4(aq) as the eluent at a flow rate of 0.25 mL/min with a d*n*/d*c* value of 0.160 mL/g for PDMAEA, which was calculated by the instrument. PDMAEA samples were dissolved in the eluent at 20 mg/mL. Detection was achieved with a Spectra-Physics 2000 instrument and an Optilab DST RI detector at ambient temperature and Wyatt DAWN DSP multiangle laser light scattering detector (λ = 633 nm). Matrix-assisted laser desorption ionization time-of-flight mass spectrometry (MALDI-ToF MS) was employed in the experimental molecular weight determination of PAA samples. The PAA samples were prepared at 5 mg/mL in deionized ultrafiltered water according to a literature procedure.[30] Measurements were performed using a Voyager-DE STR Applied Biospectrometry workstation MALDI-TOF MS setup with a triple-frequency Nd:YAG laser using negative ion analysis in linear mode with a 200 ns delay, at 25 kV, and 85% grid voltage. XPS measurements were performed on a Physical Electron 5800 ultrahigh-vacuum XPS-Auger spectrometer at Colorado State University. The incidence angle of X-ray was 45° with respect to surface normal. Atomic percentages were adjusted by removing contributions of oxygen from silicon oxide.

Results and Discussion

Recent developments in LRP techniques, namely ATRP and RAFT polymerization, have allowed for the formation of well-defined, narrow PDI polymers with a wide array of architectures by simple, versatile routes. These characteristics lend LRP techniques to be ideal in the formation of polymer brushes with high grafting densities, uniform thicknesses, and complex architectures. ATRP is arguably the most widely used LRP technique in the formation of polymer brushes but has limitations regarding functionality of monomers.[5,7] Chelating effects of monomers in ATRP, such as acrylic acid, have led researchers to form well-defined PAA brushes via postpolymerization modification routes, such as acid hydrolysis and thermal cleavage.[8–10] Because of the versatility of RAFT polymerization techniques in the polymerization of highly functional monomers, there has been increasing attention of its utilization to form well-defined functional polymer brushes. An approach of particular interest takes advantage of the vast knowledge of surface-initiated ATRP by converting surface-immobilized ATRP initiators or polymers into RAFT agents.[6,15] Recent work published by our group introduced a novel method for the immobilization of a RAFT agent onto a silicate surface for the preparation of well-defined diblock copolymer brushes using RAFT polymerization.[6] To achieve this, a traditional ATRP initiator was first immobilized on the surface and then converted to a RAFT agent using a modified ATA reaction. By taking advantage of this simple method, the versatility of RAFT polymerization to polymerize a wide variety of functional monomers and ATRPs utility in forming well-defined polymers, stimuli-responsive polymer brushes can be formed utilizing a combination of ATRP and RAFT polymerization techniques. In this case, the stimuli-responsive nature of the prepared block copolymer brushes was evaluated by introduction to a selective solvent to stimulate conformational rearrangement of the brush.

Formation of Homopolymer Brushes on Flat Silicon Substrates via Surface-Initiated ATRP. An illustration of the general synthesis route for formation of homopolymer brushes via ATRP, subsequent transformation to macro-RAFT agent, and RAFT polymerization to form diblock copolymer brushes is shown in Scheme 1. First, BMP TCS was immobilized onto a cleaned silicon wafer surface by a self-assembled process. BMP TCS has been widely used for the preparation of polymer brushes via the "grafting from" technique using ATRP.[5,6,31] As such, the preparation and deposition of this initiator have been well studied. Confirmation of the deposition of BMP TCS was achieved by ellipsometry (Table 1), goniometry (Table 1), GATR-FTIR (Figure 1a), and XPS (Table 2). Ellipsometry data for the immobilized BMP TCS showed a slight variability in the thickness, ranging from 1.5 to 3.4 nm. This was attributed to the fact that the "anchoring group" for BMP TCS is a trichlorosilane, which is prone to undergo some degree of surface cross-linking, as has been previously reported.[32] Contact angles for the BMP TCS initiator layers were relatively uniform and compared well with those shown in the literature.[5–7] A representative GATR-FTIR spectrum of the immobilized BMP TCS (Figure 1a) shows peaks at approximately 2850 and 2930 cm^{-1}, which are assigned to CH_2 stretching and C−H stretching vibrations, respectively, and at approximately 1740 cm^{-1}, which is assigned to the carbonyl stretching vibration of the ester group. XPS analysis of the immobilized BMP TCS (Table 2) verifies the presence of bromine (Br 3d), carbon (C 1s), and oxygen (O 1s). There is a small amount of variation in the atomic percentage of bromine for each deposition. This is attributed to the error introduced into these measurements by the calculation used to remove the Si peak from the spectra to give the adjusted atomic percentages. However, while there is variation of the atomic percentage of bromine between different samples, variation across the surface of each sample is negligible.

Once the bromosilane deposition was characterized, homopolymer brushes of PSty and PMA were prepared via surface-initiated ATRP. In each case, free initiator, E2-BiB, was

Table 1. Thickness[b] and Contact Angle[c] Data for Diblock Copolymer Brushes Synthesized by a Combination of ATRP and RAFT Surface Polymerizations, along with Corresponding Molecular Weight Properties[d] of Solution Polymerizations

		contact angle data[c]		molecular weight (g/mol)		
surface structure[a]	Δ thickness (nm)[b]	$\theta_{advancing}$	$\theta_{receding}$	$M_{n(theory)}$[d]	$M_{n(exper)}$[e]	PDI[e,f]
bromosilane initiator	3	80	71			
PSty (ATRP)	5.2	90	82	5735	5240[e]	1.05
PSty after ATA with Cu(0)	−0.1	89	81			
PSty (ATRP)-*b*-PSty (RAFT)	5.7	92	83	5468	5342[e]	1.11
bromosilane initiator	3.4	83	71			
PSty (ATRP)	9.9	90	79	11468	11345[e]	1.05
PSty after ATA with Cu(0)	0.3	94	81			
PSty (ATRP)-*b*-PNIPAM (RAFT)	3.0	72	58	8733	8606[e]	1.12
bromosilane initiator	1.9	84	74			
PSty (ATRP)	8.3	95	85	8236	8103	1.08
PSty after ATA with tin(II) 2-ethylhexanoate	−0.2	94	80			
PSty (RAFT)-*b*-PSty (RAFT)	3.9	96	89	4395	4657[e]	1.08
bromosilane initiator	1.8	84	74			
PSty (ATRP)	8.1	95	83	8236	8103[e]	1.08
PSty after ATA with tin(II) 2-ethylhexanoate	0.3	94	80			
					10840[g]	
PSty (ATRP)-*b*-PAA (RAFT)	7.4	33	27	14335		
					10888[h]	1.10[h]
bromosilane initiator	1.5	74	59			
PMA (ATRP)	5.3	63	50	12335	13963[e]	1.21
PMA after ATA with tin(II) 2-ethylhexanoate	−0.6	67	53			
PMA (RAFT)-*b*-PDMAEA (RAFT)	3.1	48	36	17451	15120[e]	1.25

[a] PSty = poly(styrene), ATRP = atom transfer radical polymerization, ATA = atom transfer addition, RAFT = reversible addition−fragmentation chain transfer polymerization, PNIPAM = poly(*N*-isopropylacrylamide), PAA = poly(acrylic acid), PMA = poly(methyl acrylate), and PDMAEA = poly(*N,N*-(dimethylamino)ethyl acrylate). [b] Thicknesses were determined by ellipsometry and are an average of five samplings across the sample. Error of thicknesses measured was within ±0.5 nm. [c] Static, advancing, and receding contact angles were taken at 0° and 35° using goniometry and are an average of five samplings across the sample. The standard deviation of contact angles was less than 2°. [d] Theoretical number-average molecular weight (M_n) for ATRP systems calculated using the equation M_n = (molecular weight of initiator) + (molecular weight of monomer) × ([monomer]$_0$/[initiator]$_0$) × (monomer conversion) and M_n for RAFT polymerizations calculated using the equation M_n = (molecular weight of RAFT agent) + (molecular weight of monomer) × ([monomer]$_0$/[RAFT agent]$_0$) × (monomer conversion), where molecular weight is representative of the outermost block only, as only homopolymers were formed in solution. [e] Characterized via gel permeation chromatography. [f] PDI = polydispersity index (= M_w/M_n). [g] Characterized via end-group analysis by ^{1}H NMR. [h] Determined by MALDI-ToF MS.

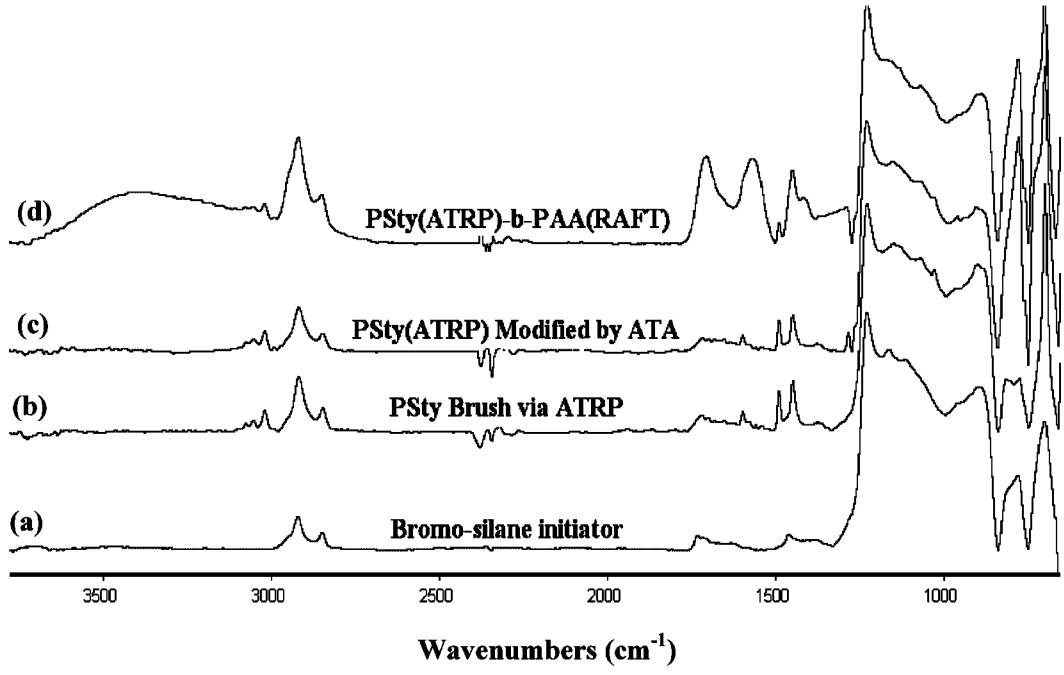

Figure 1. Representative grazing angle attenuated total reflectance−Fourier transform infrared spectrum for the (a) deposition of (11-(2-bromo-2-methyl)propionyloxy)undecyltrichlorosilane, (b) formation of poly(styrene) (PSty) homopolymer brush via atom transfer radical polymerization, (c) conversion to a PSty macro-RAFT agent through a modified atom transfer addition reaction, and (d) PSty-*b*-poly(acrylic acid) diblock copolymer brush.

added to the polymerization system to ensure control of the polymerization. It has been reported that the addition of sacrificial or free initiator is required to provide a sufficiently high concentration of deactivator, copper(II) species, which is necessary for the formation of well-defined polymers of controlled molecular weight.[33] Without sufficient concentration of deactivator in solution, the polymerization will not be controlled and nonuniform films will be produced. Additionally, introduction of free initiator allows for formation of free polymer in solution, the properties of which have been shown to correlate with the polymer attached to the surface.[26] Since insufficient amounts of polymer can be degrafted from flat silicon surfaces

Table 2. Adjusted[a] Atomic Percentage of Polymer Modified Surfaces and Selective Solvent Treatment of Diblock Copolymer Brushes from Wide-Scan X-ray Photoelectron Spectroscopy (XPS)

	wide-scan XPS data[a]				
surface structure	C 1s	O 1s	Br 3d	S 2s	N 1s
bromosilane initiator	70.3	27.2	2.6		
PSty (ATRP)	93.6	6.0	0.3		
PSty after ATA with Cu(0)	97.4	0.8	<0.1	1.8	
PSty (ATRP)-*b*-PSty (RAFT)	99.4	<0.1		1.2	
bromosilane initiator	67.6	29.6	2.8		
PSty (ATRP)	96.0	3.9	0.1		
PSty after ATA with Cu(0)	96.8	2.7	<0.1	0.5	
PSty (ATRP)-*b*-PNIPAM (RAFT)	90.6	6.6		0.3	2.5
selective solvent study with cyclohexane	92.8	5.5		0.2	1.6
bromosilane initiator	64.2	33.5	2.3		
PSty (ATRP)	97.9	0.4	1.8		
PSty after ATA with tin(II) 2-ethylhexanoate	93.8	5.0	<0.1	1.0	
PSty (RAFT)-*b*-PSty (RAFT)	99.5	<0.1		0.3	
bromosilane initiator	66.7	31.6	1.8		
PSty (ATRP)	97.7	2.1	0.2		
PSty after ATA with tin(II) 2-ethylhexanoate	97.6	2.1	<0.1	0.3	
PSty (ATRP)-*b*-poly(acrylic acid) (RAFT)	89.6	10.0		0.4	
selective solvent study with cyclohexane	98.0	1.7		0.2	
bromosilane initiator	79.7	18.4	1.9		
PMA (ATRP)	80.1	19.7	0.2		
PMA after ATA with tin(II) 2-ethylhexanoate	76.5	22.7	<0.1	0.6	
PMA (RAFT)-*b*-PDMAEA (RAFT)	63.8	31.9		0.2	4.2
slective solvent study with dichloromethane	66.3	32.0		0.4	1.3

[a] Atomic percentages were adjusted by removing the expected percentage of oxygen and silicon brought about by the native silicon dioxide layer of silicate substrates.

for characterization, free polymer can be analyzed to provide an approximation of the molecular weight properties of the immobilized chains. Because of possible entanglement of the free polymer with immobilized chains, all samples were extracted in THF for 24 h to remove any untethered polymer chains from the surface.

PSty homopolymer brushes were synthesized using a 3.9 M solution of Sty in anhydrous anisole with a catalyst system of CuBr/PMDETA at 90 °C for either 12 or 24 h. The formation of PSty brushes was confirmed by ellipsometry (Table 1), contact angle measurements (Table 1), GATR-FTIR (Figure 1b), and XPS (Figure 2a and Table 2). Ellipsometry indicated an increased thickness of 5.2 nm after 12 h and 9.9, 8.3, and 8.1 nm after 24 h for four different PSty brushes prepared under similar conditions. The homopolymer brushes demonstrated advancing contract angles of 90°, 90°, 95°, and 95°, respectively (Table 1), which compare well with literature data for the formation of a PSty homopolymer brush synthesized via ATRP.[5,7] A representative GATR-FTIR spectrum for a PSty homopolymer brush (Figure 1b) also confirmed the presence of PSty due to the expected appearance of aromatic C−H stretching around 3100 cm^{-1} and C═C aromatic doublets at 1420−1480 cm^{-1}. All PSty homopolymer brushes exhibited similar GATR-FTIR spectra. Wide-scan XPS spectra showed a marked increase in carbon validating the existence of PSty homopolymers (Figure 2a and Table 2). The sacrificial PSty chains, for each inner block, were characterized by GPC providing monomodal molecular weight traces with experimental values correlating well to theoretical values, along with narrow PDIs (Table 1), which are characteristic of well-defined polymers prepared via ATRP. Additionally, thicknesses as determined by ellipsometry correlate well with experimental molecular weight evolution. For the PSty homopolymer brush prepared with a 12 h reaction time the molecular weight of the free polymer of 5240 g/mol compared to a thickness of 5.2 nm (Table 1). While the PSty homopolymer brushes prepared with a 24 h reaction time produced experimental molecular weights of the free polymer of 11 345, 8103, and 8103 g/mol, which correspond well to polymer brush thicknesses of 9.9, 8.3, and 8.1 nm, respectively (Table 1).

Formation of PMA homopolymer brushes via ATRP followed a similar procedure to that of PSty. As before, BMP TCS initiator was deposited giving typical values of thickness from ellipsometry, advancing and receding contact angles from goniometry, and atomic percentages from wide-scan XPS (Table 1). Surface-initiated ATRP was then employed in the formation of a PMA homopolymer brush using a 3.7 M solution of MA in anhydrous toluene with a catalyst system of CuBr/PMDETA at 95 °C for 24 h. PMA homopolymer brush synthesis was confirmed by ellipsometry (Table 1), goniometry (Table 1), GATR-FTIR spectroscopy (Figure 3), and XPS (Table 2). Ellipsometry indicated an increase in thickness of 5.3 nm for the PMA homopolymer brush (Table 1). The PMA homopolymer brush demonstrated an advancing contact angle of 63°, which is similar to literature data for PMA brush formation (Table 1).[34] GATR-FTIR spectroscopy of the PMA homopolymer brush (Figure 3b) also confirmed the presence of PMA due to the expected appearance of a large carbonyl stretching vibration at ∼1732 cm^{-1} and an increase in the asymmetric C−H stretch at ∼2920 cm^{-1}.[34] The wide-scan XPS spectrum showed an increase in both carbon and oxygen, with adjusted atomic percentage of 80.1% and 19.7%, respectively, indicating the presence of PMA on the surface (Table 2). Finally, sacrificial polymer chains indicated comparable theoretical and experimental molecular weights, 12 335 and 13 963 g/mol, respectively, confirming controlled ATRP in solution (Table 1).

Conversion of Surface Immobilized Macro-ATRP Initiator to a Terminal RAFT Moiety. Once formation of the PSty homopolymer brushes had been confirmed, a modified ATA reaction was used to convert the terminal bromine end groups to macro-RAFT agents (Scheme 1). The conversion was carried out under oxygen-free conditions in the presence of CuBr, Cu(0), PMDETA, and DTBDS at 85 °C for 48 h. A similar procedure was followed by Tsujii and co-workers; however, without addition of deactivator, controlled extension to form diblock brushes with RAFT polymerization was unsuccessful.[15] Recently, our group reported the addition of Cu(0) was critical for efficient conversion of the surface immobilized bromine end group of BMP TCS to the dithiobenzoate RAFT agent.[6] As such, conversion of the PSty terminal bromine end groups to the RAFT agent was performed with a 1.5-fold excess of Cu(0) to Cu(I) and a large excess of DTBDS. The excess of DTBDS is used to maximize the probability that the radical generated by activation of the immobilized macro-ATRP initiator will undergo reaction with the DTBDS, thus forming the surface immobilized macro-RAFT agent (Scheme 1). Ellipsometry data showed changes in thicknesses after reaction with the DTBDS ranging between −0.6 and 0.3 nm (Table 1). Negligible changes in thickness were expected in this reaction as the large bromine atom is being replaced with a dithiobenzoate structure. The negative changes in thickness observed are within error of the instrument used for these measurements and thus really only indicate an insignificant change in thickness. Goniometry showed negligible changes in the advancing contact angle, ranging from −1° to 4°, after conversion to the macro-RAFT agent. A representative GATR-FTIR spectrum of the PSty

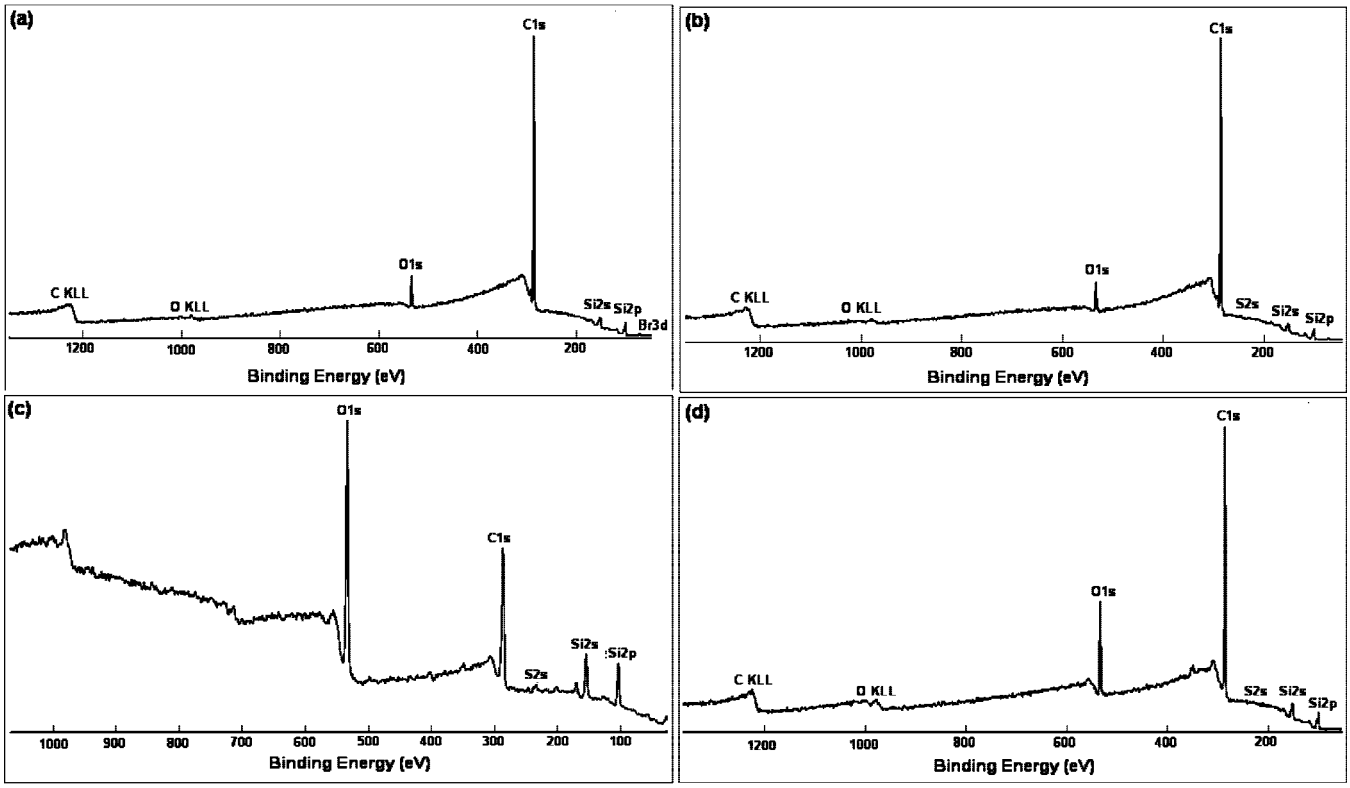

Figure 2. Wide-scan X-ray photoelectron spectroscopy of (a) poly(styrene) (PSty) homopolymer brush synthesized via surface-initiated atom transfer radical polymerization (ATRP), (b) PSty-modified macro-RAFT agent, (c) PSty-*b*-poly(acrylic acid) (PAA) diblock copolymer brush, and (d) rearrangement of PSty-*b*-PAA diblock copolymer brush after being subjected to cyclohexane.

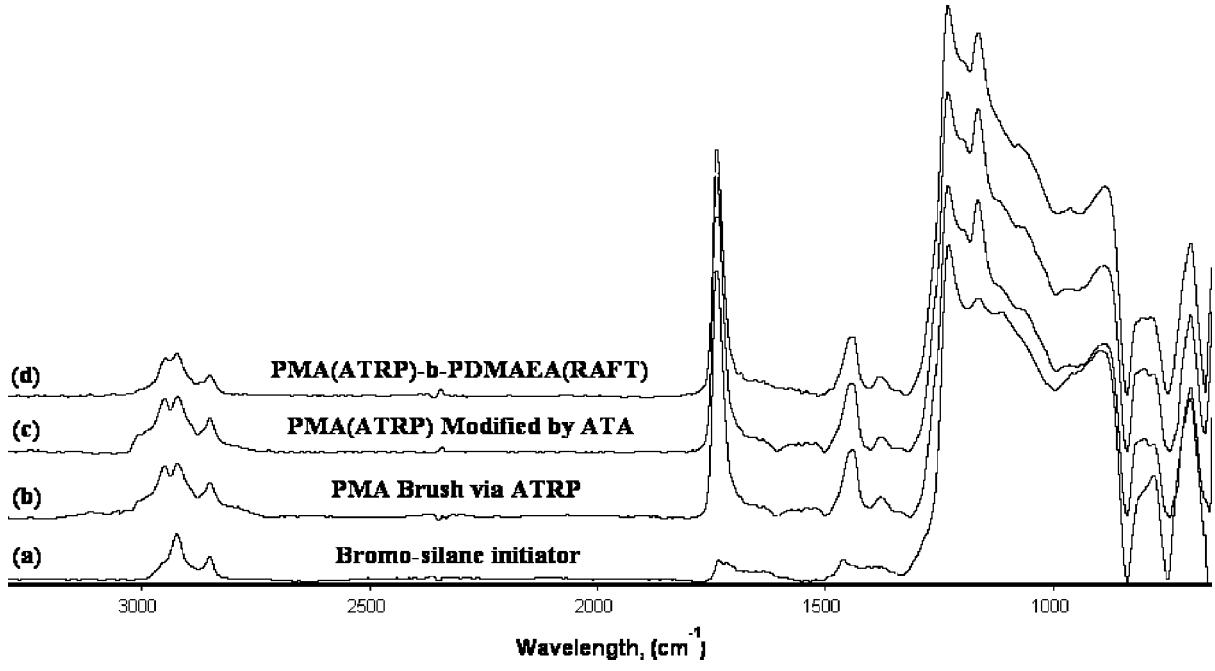

Figure 3. Representative attenuated total reflectance−Fourier transform infrared spectrum for the (a) deposition of (11-(2-bromo-2-methyl)propionyloxy)undecyltrichlorosilane, (b) formation of poly(methyl acrylate) (PMA) homopolymer brush via atom transfer radical polymerization, (c) conversion to a PMA macro-RAFT agent through a modified atom transfer addition reaction, and (d) PMA-*b*-poly(*N,N*-(dimethylamino)ethyl acrylate) diblock copolymer brush.

homopolymer brush, prepared via surface-initiated ATRP, after reaction with the DTBDS (Figure 1c) indicates few discernible differences to that of the original PSty homopolymer brush spectra. We attribute this to the very low concentration of RAFT agent groups present at the surface. Wide-scan XPS was also collected for each homopolymer brush before and after ATA modification to compare atomic percentages of bromine and sulfur (Table 2). The proposed modified ATA conversion reaction gives a theoretical ratio of two sulfur atoms for every one bromine atom present on the immobilized BMP TCS (Scheme 1). However, calculations did not demonstrate the theoretical ratio of sulfur to bromine, but instead a range of atomic percentages from 1.5 to 6 atom % was seen. This range and deviation from theoretical calculations were attributed to

chain-end exclusion effects from the homopolymer brushes. Even though theoretical ratios were not evident in all systems, in each case the atomic percentage of bromine (Br 3d) decreased to <0.1 after reaction with DTBDS, indicating the removal of the Br end groups from the ATRP macroinitiator, with a concurrent appearance of sulfur (S 2s) in the XPS (Table 2).

Sequential Addition for Preparation of Diblock Copolymer Brushes via RAFT Polymerization. Following the ATA reactions on the homopolymer brushes, RAFT polymerization was used to synthesize a range of diblock copolymer brushes in order to demonstrate the ability to convert a macro-ATRP initiator to macro-RAFT agent. Diblock copolymer brushes, PSty-*b*-PSty, PSty-*b*-PAA, and PSty-*b*-PNIPAM, were formed by employing homopolymer brushes of PSty synthesized via surface-initiated ATRP then modified to produce macro-RAFT agents. The surface-initiated RAFT polymerizations involved the addition of an initiator, AIBN, and free RAFT agent, DATC, to mediate synthesis of the outer blocks and also resulted in the production of free polymer in solution. Furthermore, the addition of free RAFT agent should assist in suppressing radical−radical coupling reactions on the surface by providing preferential reaction of surface bound radicals with free RAFT agent. By minimizing any termination reactions, the chain-end functionality of the surface-immobilized polymers is preserved, allowing for the formation of diblock copolymer brushes with uniform film thickness.

The diblock copolymer brushes were characterized using ellipsometry, goniometry, GATR-FTIR spectroscopy, and XPS. Initially, a PSty-*b*-PSty diblock copolymer brush was synthesized to demonstrate the effectiveness of the ATA reaction at converting macro-ATRP initiators to macro-RAFT agents. As expected, the contact angles (Table 1) and GATR-FTIR spectrum of the diblock copolymer brush showed no discernible differences after the chain extension using RAFT polymerization. However, an increase of 5.7 nm in thickness confirmed extension of the initial PSty brush to form a diblock copolymer brush utilizing the combination of surface-initiated ATRP and RAFT polymerization techniques (Table 1). In addition, wide-scan XPS showed a decrease in oxygen and subsequent increase in carbon atomic percentage with the PSty outer block extension via surface-initiated RAFT polymerization, indicating a thicker layer of PS had been formed on the surface (Table 2). Free polymer chains formed by the addition of free RAFT agent were isolated and characterized by GPC affording monomodal molecular weight distributions with an experimental value correlating well to theoretical values, along with narrow PDIs, which are characteristic of well-defined polymers prepared via RAFT (Table 1). The experimental molecular weight of the PSty formed via RAFT polymerization of 5342 g/mol also correlated well with the respective polymer brush thickness of 5.7 nm. This also compared well to the formation of the first PSty block by ATRP, where a molecular weight of 5240 g/mol corresponded to a thickness of 5.2 nm. It should be noted that in the preparation of all of the diblock copolymer brushes polymerization to produce the second block only results in the formation of a homopolymer in solution, not a diblock. The reason for this is that a standard RAFT agent is employed in solution for the polymerization, not a macro-RAFT agent prepared from the free polymer of the first block.

The next diblock copolymer brush synthesized was PSty-*b*-PNIPAM, which was formed from an ATA-modified PSty homopolymer brush, prepared via ATRP, followed by surface-initiated RAFT polymerization of NIPAM. Formation of the PNIPAM block was confirmed by ellipsometry, where a thickness increase of 3.0 nm from that of the initial homopolymer brush of PSty was observed (Table 1). Decreases in advancing contact angle measurements, from 94° to 72°, additionally confirmed the successful formation of the diblock copolymer brush, as PNIPAM is more hydrophilic in nature than PSty.[35] The GATR-FTIR spectrum demonstrated a broad stretch above 3300 cm^{-1} and small stretch at 1640 cm^{-1}, indicating the presence of the acrylamide functionality; an increase in intensity of the $-CH_2$ stretching and C−H stretching vibrations between 2800 and 3000 cm^{-1} due to backbone methylenes; a peak at 1720 cm^{-1} assigned to the carbonyl stretch of the amide; and a stretch at 1380 cm^{-1} attributed to the addition of $-CH_3$ and isopropyl groups, which is comparable to PNIPAM films discussed in the literature.[36] In addition, the wide-scan XPS spectrum showed the appearance of nitrogen, 2.5 atomic %, after the diblock copolymer extension, which was attributed to the amide functionality present in the NIPAM monomer (Table 2). Furthermore, theoretical and experimental molecular weights correlated well in conjunction with a low PDI, indicating the RAFT polymerization of NIPAM in solution was controlled (Table 1). However, the PNIPAM thickness increase of 3.0 nm did not appear to correlate well with the experimental PNIPAM molecular weight of 8606 g/mol. These results suggest that the PNIPAM is less controlled from the surface in comparison to in solution due to the relatively small increase in thickness on the surface for the experimental molecular weight of the free polymer. This discrepancy may be attributed to either surface termination during the RAFT polymerization or loss of end-group functionality after homopolymer brush formation and the ATA reaction.

Preparation of Surface-Immobilized Macro-RAFT Agents Utilizing a Tin(II) 2-Ethylhexanoate/PMDETA Catalyst System. Although the Cu(0)/CuBr/PMDETA catalyst system has proven successful with the ATA-modified conversion of surface-immobilized ATRP initiators to RAFT agents and the formation of a variety diblock copolymer brushes,[6] recent work by the Matyjaszewski group has utilized other reducing agents, such as ascorbic acid and tin(II) 2-ethylhexanoate, in the development of novel ATRP systems based upon activators regenerated by electron transfer (ARGET).[37–39] These reducing agents are especially advantageous as they are both FDA approved and also overcome issues associated with removal of copper metal catalysts due to the small amounts of oxidatively stable Cu(II) complexes that are required to successfully control the ARGET polymerization.[38] Because of the ability of these reducing agents to quickly and efficiently convert Cu(II) species to Cu(I), their use in the ATA modification step may provide a more versatile modification route to form either surface-immobilized RAFT agents or macro-RAFT agent terminated chains. As such, we have made use of a tin(II) 2-ethylhexanoate/CuBr/PMDETA catalyst system for the modified ATA reaction (Scheme 1).

Initially, the modified ATA reaction was utilized to form a PSty-*b*-PSty diblock copolymer brush employing the tin(II) 2-ethylhexanoate/CuBr/PMDETA catalyst system. First, BMP TCS initiator was deposited giving typical values of thickness from ellipsometry, advancing and receding contact angles, and atomic percentages from wide-scan XPS (Tables 1 and 2). Homopolymer brushes of PSty with thicknesses of 8.3 and 8.1 nm were then formed via ATRP, by the previously discussed methods, both providing increased advancing contact angles of 95°, attributed to the hydrophobic nature of PSty (Table 1). Each GATR-FTIR spectrum for the PSty homopolymer brushes also validated the presence of PSty due to the expected appearance of aromatic C−H stretching around 3100 cm^{-1} and C═C aromatic doublets at 1420−1480 cm^{-1}. Wide-scan XPS spectra showed a marked increase in carbon, confirming the formation of PSty homopolymer brushes (Table 2). Free polymer was isolated from solution and characterized by GPC, affording monomodal molecular weight distributions with an experimental molecular weight value correlating well with theoretical values

along with narrow PDIs (Table 1). The experimental molecular weights of the PSty formed via ATRP also correlated well with the respective polymer brush thicknesses.

The bromine macroinitiator of the PSty homopolymer was then converted to the dithioester macro-RAFT agent through the modified ATA reaction with a catalyst system at a 1:3.3:6 molar ratio of CuBr/tin(II) 2-ethylhexanoate/PMDETA. Ellipsometry and goniometry data showed negligible changes in thickness and contact angles after conversion to the surface immobilized macro-RAFT agent (Table 1). Additionally, as previously discussed, GATR-FTIR spectra after conversion provided little information on changes in surface functionality. As such, XPS was employed in order to monitor the conversion of bromine end groups to the dithioester functionality with the use of the CuBr/tin(II) 2-ethylhexanoate/PMDETA catalyst system. After the new ATA reaction, the XPS spectra showed a disappearance of bromine, attributed to the macro-ATRP initiator, with a simultaneous appearance of sulfur, owing to conversion to the macro-RAFT agent (Table 2). In order to confirm the presence of the RAFT agent end groups on the PSty homopolymer brush, the subsequent RAFT polymerization of styrene allowed for the formation of a PSty-*b*-PSty diblock copolymer brush. The addition of the PSty outer block by RAFT polymerization was confirmed by an increase in thickness of 3.9 nm (Table 1). Nominal changes in contact angles and GATR-FTIR spectrum were seen (Table 1); however, an increase in carbon atomic percentage of 6.0% from wide-scan XPS characterization (Table 2) provided further evidence of PSty block copolymer formation. Furthermore, GPC characterization of the free polymer demonstrated a monomodal molecular weight distribution, good agreement between theoretical and experimental molecular weights, and a narrow PDI of 1.08, confirming control of the solution RAFT polymerization (Table 1). The experimental molecular weight of 4657 g/mol correlated well with an increase in thickness of 3.9 nm.

The tin(II) 2-ethylhexanoate/CuBr/PMDETA catalyst system was also employed in the synthesis of the diblock copolymer brush, PSty-*b*-PAA. In this case, a PSty homopolymer brush prepared via ATRP was converted to a macro-RAFT agent using the new ATA reaction, and the PAA block was then directly formed by RAFT polymerization of AA. The PSty-*b*-PAA diblock copolymer brush formation was confirmed using the standard characterization techniques. Ellipsometry indicated a thickness increase of 7.4 nm from that of the original PSty homopolymer brush of 8.1 nm (Table 1). Goniometry demonstrated a decrease in advancing contact angle from 94° to 33° (Table 1). The decrease in advancing contact angle is expected due to the more hydrophilic nature of PAA when compared to PSty.[8] The GATR-FTIR spectrum also confirmed formation of the PAA block (Figure 1d) with the appearance of a broad stretch between 3000 and 3600 cm^{-1} attributed to $-OH$ stretching of the carboxylic acid, along with carbonyl stretching vibrations due to the carboxylic acid and unprotonated carboxylate functionalities at 1705 and 1575 cm^{-1}, respectively. To further confirm the presence of the PAA block, the wide-scan XPS spectra of the PSty-*b*-PAA diblock copolymer brush showed an increased atomic percentage of oxygen from 2.1 to 10.0 atom % attributed to the addition of the acid functionality in the AA monomer. Despite several attempts at GPC characterization, poor elution behavior of the PAA sample provided no useful information on the experimental molecular weight characteristics. As such, molecular weight analysis of the free PAA from solution was achieved by a combination of ^1H NMR and MALDI-ToF MS. End-group analysis via ^1H NMR provided an experimental molecular weight of 10 840 g/mol by comparing the area of the terminal $-CH_3$ peak, attributed to the DATC RAFT agent, to the total methylene signal from the PAA backbone. MALDI-ToF MS provided a comparable molecular weight of 10 888 g/mol with a PDI of 1.10. These results demonstrate the well-defined nature of the PAA prepared via RAFT polymerization due to the low PDI and a comparable experimental and theoretical molecular weight value (Table 1). In addition, the experimental molecular weight for the PAA correlated well with the increase in thickness of 7.4 nm. To the best of our knowledge, this is the first example of the formation of a well-defined PSty-*b*-PAA diblock copolymer brush by LRP techniques, without the addition of postpolymerization modification steps or micropatterning.

Finally, the tin(II) 2-ethylhexanoate/CuBr/PMDETA catalyst system was employed for the modified ATA reaction involving a PMA homopolymer brush formed via ATRP. Following PMA homopolymer brush formation, the bromine end groups were converted to a macro-RAFT agent through a modified ATA reaction utilizing a catalyst system with a molar ratio of 6:1:3:3 PMDETA/CuBr/tin(II) 2-ethylhexanoate As previously discussed, changes in thickness, contact angles, and the GATR-FTIR spectrum were negligible (Table 1). The wide-scan XPS spectrum showed the disappearance of bromine and a subsequent appearance of sulfur verifying conversion to the macro-RAFT agent (Table 2). To confirm the activity of the macro-RAFT agent, a PMA-*b*-PDMAEA diblock copolymer brush was formed via RAFT polymerization of DMAEA. The PDMAEA outer block was produced by employing a 3.0 M solution of DMAEA in anhydrous toluene with DATC and AIBN at 60 °C for 12 h. Ellipsometry indicated a thickness increase of 3.1 nm from that of the initial PMA macro-ATRP initiator surface after surface-initiated RAFT polymerization of DMAEA (Table 1). Decreases in advancing contact angle measurements, from 67° to 48°, additionally confirmed successful extension to form the diblock copolymer brush, as PDMAEA is more hydrophilic in nature in comparison to PMA. While the GATR-FTIR spectrum (Figure 3d) shows a slight shift in the ratio of the CH_2 stretches at ~2920 cm^{-1}, which is attributed to the addition of the PDMAEA block, the characteristic peaks for the $-N(CH_3)_2$, which generally appear at ~2830 cm^{-1}, seem to be overlapping with peaks from the PMA homopolymer layer. The GATR-FTIR spectrum also demonstrated a slight increase in intensity of the carbonyl stretch at 1720 cm^{-1}, indicating the addition of a PDMAEA block. In addition, the wide-scan XPS spectra showed an appearance of nitrogen, 4.2 atomic %, after the diblock copolymer extension, attributed to the presence of the amide functionality in the PDMAEA block. Free PDMAEA formed by the addition of free RAFT agent was isolated and characterized by GPC. The experimental molecular weight value correlated well with the theoretical value and the PDI was also low, confirming the controlled nature of the RAFT polymerization in solution (Table 1). Once again, it appears that the PDMAEA polymerization in solution was more controlled than that from the surface due to the fact that the experimental molecular weight of 15 120 g/mol only corresponded to a thickness increase of 3.2 nm. This discrepancy may be attributed to either surface termination or loss of end-group functionality after homopolymer brush formation, limiting an increase in the thickness of the diblock copolymer brush.

Determination of the Stimuli Responsive Nature of the Diblock Copolymer Brushes through Selective Solvent Treatment. Formation of diblock copolymer brushes via LRP techniques and use of selective solvent treatment to induce a stimuli response have been widely studied.[5,7,21,24] The interactive behavior of block copolymer brushes in solvents is of particular interest because of the possibility of microphase separation due to the inner block being covalently bound to the substrate. The stimuli-responsive nature of the PSty-*b*-PAA, PSty-*b*-PNIPAM, and PMA-*b*-PDMAEA diblock copolymer brushes was il-

Table 3. Contact Angle Data[b] for Selective Solvent Treatment of Diblock Copolymer Brushes

surface structure[a]	solvent	contact angle data[b] $\theta_{advancing}$	$\theta_{receding}$
PSty-*b*-PAA	first *N,N*-dimethylformamide	33	27
	first cyclohexane	58	50
	second *N,N*-dimethylformamide	39	31
	second cyclohexane	63	42
PSty-*b*-PNIPAM	first *N,N*-dimethylformamide	62	49
	first cyclohexane	68	57
	second *N,N*-dimethylformamide	65	55
	second cyclohexane	78	65
PMA-*b*-PDMAEA	first toluene	48	32
	first dichloromethane	57	53
	second toluene	49	32
	second dichloromethane	58	53

[a] PSty = poly(styrene), PAA = poly(acrylic acid), PNIPAM = poly(*N*-isopropylacrylamide), PMA = poly(methyl acrylate), and PDMAEA = poly(*N,N*-(dimethylamino)ethyl acrylate). [b] Static, advancing, and receding contact angles were taken at 0° and 35° using goniometry and are an average of five samplings across the sample. The standard deviation of contact angles was less than 2°.

Table 4. Solubility Parameters of Polymers[a]

polymer[b]	δ $(J/cm^3)^{1/2}$	polymer[b]	δ $(J/cm^3)^{1/2}$
PSty	19.6	PMA	19.2
PAA	16.2	PDMAEA	19.8
PNIPAM	25.5		

[a] Solubility parameters were calculated utilizing the group contribution method published by Van Krevelen.[29] [b] PSty = poly(styrene), PAA = poly(acrylic acid), PNIPAM = poly(*N*-isopropylacrylamide), PMA = poly(methyl acrylate), and PDMAEA = poly(*N,N*-(dimethylamino)ethyl acrylate).

lustrated through a series of selective solvent studies. In the first diblock copolymer brush system, PSty-*b*-PAA, DMF was chosen as a good solvent for both blocks to effectively extend the entire brush structure, providing an initial advancing water contact angle of 33° (Table 3), similar to that shown in literature for PAA thin films.[5] The extended brush was then subjected to a solvent change using cyclohexane, a nonsolvent for PAA. Because cyclohexane is a good solvent for PSty, but a nonsolvent for PAA, the outer PAA block should attempt to move away from the solvent, while the inner PSty block should attempt to move to the surface.[5] With the addition of cyclohexane, some degree of rearrangement was confirmed by an increase in the advancing contact angle from 33° to 58° (Table 3), attributed to the more hydrophobic PSty block being situated at the air−water interface. Wide-scan XPS data for the rearrangement of PSty-*b*-PAA showed an increase in carbon atomic percentage from 89.6 to 98.0 atom %, with a respective decrease in oxygen atomic percentage from 10.0 to 1.7 atom %, further confirming at least partial rearrangement of the PSty inner block to the polymer−air interface (Table 2). The process of gradual solvent change was repeated three times, providing similar results each time, which demonstrates the reversibility of the rearrangement.

The contact angle results from the solvent switching suggest that the PSty-*b*-PAA diblock copolymer brush did not completely rearrange as PSty is known to have an advancing contact angle of ~90°−95°. However, the rearrangement of block copolymer brushes can be affected by several factors including chain architecture, grafting density, composition of the chains, and overall molecular weight.[5] Lower than expected contact angle values for the DMF−cyclohexane solvent switching study for the PSty-*b*-PAA diblock copolymer brush are attributed to large solubility parameter, δ, value differences between PAA and PSty, resulting in incomplete rearrangement, which has been previously discussed in literature (Table 4).[5] It has been speculated that the incomplete rearrangement of diblock copolymer brushes, due to large δ differences between the blocks, produces structures which have varying amounts of both the inner and outer block at the interface, depending on the magnitude of the difference in the δ values.[21,24] Additionally, in the case of the PSty-*b*-PAA diblock copolymer brush, the thickness of the PAA outer block is approximately the same as the PSty inner block, which may result in steric factors also contributing to the incomplete rearrangement of the brush.

Next, the stimuli-responsive nature of the PSty-*b*-PNIPAM diblock copolymer brush was examined through selective solvent treatment. Again, DMF was chosen as a good solvent for both blocks and cyclohexane as a nonsolvent for the PNIPAM outer block, but a good solvent for the PSty inner block. Contact angles were determined through goniometry after each solvent switch (Table 3). An advancing contact angle of 62° was achieved after extension of both blocks in DMF (Table 3). Change over to cyclohexane provided at least partial rearrangement of the block copolymer brush, yielding an increase in the advancing contact angle to 78° which was attributed to the more hydrophobic PSty inner block being at the polymer−water interface (Table 3). Once again, the reversible nature of the rearrangement due to solvent interactions was confirmed by repeating the gradual solvent switching three times, with similar results seen each time (Table 3). Wide-scan XPS spectra further confirmed rearrangement of the PNIPAM inner block with a decrease in nitrogen from 2.5 to 1.6 atom % and oxygen from 6.6 to 5.5 atom % (Table 2). As with the previous example, both goniometry and XPS results suggest incomplete rearrangement of the diblock copolymer brush which is again attributed to a large difference in δ values of PSty and PNIPAM (Table 4).

Lastly, the PMA-*b*-PDMAEA diblock copolymer brush was subjected to selective solvent treatments. Toluene was selected as the good solvent for extension of both the PMA and PDMAEA blocks, while dichloromethane was used as the nonsolvent for the outer PDMAEA block but a good solvent for the inner PMA block. Goniometry measurements after extension of the diblock copolymer brush yielded an advancing contact angle of 48°. Solvent change over to dichloromethane resulted in the advancing contact angle increasing to 57°, confirming at least partial rearrangement of the diblock copolymer brush. Again, the rearrangement capability due to solvent parameters was completely reversible after three cycles of gradual solvent switching (Table 3). In this case, the advancing contact angles before and after switching were very close to the contact angles for PDMAEA and PMA, respectively (Tables 2 and 3). This result suggest that the PMA-*b*-PDMAEA diblock copolymer brush undergoes more complete rearrangement, which is attributed to a smaller δ value difference between PMA and PDMAEA (Table 4). The closer δ values allow for more favorable interactions between the two blocks, permitting the formation of a stimuli-responsive diblock copolymer brush.

Conclusions

This research has demonstrated the utilization of a combination of both ATRP and RAFT polymerization techniques in the formation of a range of well-defined diblock copolymer brushes including PSty-*b*-PAA, PSty-*b*-PNIPAM, and PMA-*b*-PDMAEA. A modified ATA reaction was utilized to exchange the bromine end group of a macro-ATRP initiator to form a surface-immobilized macro-RAFT agent, which was successfully chain extended via RAFT polymerization to produce diblock copolymer brushes. Both Cu(0) and tin(II) 2-ethylhexanoate were employed in the modified ATA reaction step to provide a more versatile route in formation of macro-RAFT agents for the synthesis of functional polymer brushes via RAFT polymerization. For the first time, we have provided a route for the

formation of well-defined PAA diblock copolymer brushes without the use of postpolymerization modification. Furthermore, selective solvent treatment of the PSty-*b*-PAA, PSty-*b*-PNIPAM, and PMA-*b*-PDMAEA diblock copolymer brushes, formed through a combination of surface-initiated ATRP and RAFT polymerizations, showed rearrangement capabilities in response to solvent changes.

Acknowledgment. This research was supported by the Air Force Office of Scientific Research (FA9550-08-1-0007). The authors also thank Prof. Brent Sumerlin of Southern Methodist University and Prof. Charles McCormick of the University of Southern Mississippi for assistance with GPC data collection.

References and Notes

(1) Matyjaszewski, K.; Davis, T. P. *Handbook of Radical Polymerization*; Wiley-Interscience: New York, 2002.
(2) Moad, G.; Solomon, D. H. *The Chemistry of Radical Polymerization*, 2nd fully revised ed.; Elsevier Ltd.: Amsterdam, 2006.
(3) Matyjaszewski, K.; Xia, J. *Chem. Rev.* **2001**, *101*, 2921–2990.
(4) Perrier, S.; Takolpuckdee, P. *J. Polym. Sci., Part A: Polym. Chem.* **2005**, *43*, 5347–5393.
(5) Jordan, R., Ed. *Surface Initiated Polymerization I and II: Advances in Polymer Science*; Springer: Berlin, 2006.
(6) Rowe-Konopacki, M. D.; Boyes, S. G. *Macromolecules* **2007**, *40*, 879–888.
(7) Advincula, R. C.; Brittain, W. J.; Caster, K. C.; Ruhe, J. *Polymer Brushes: Synthesis, Characterization, Applications*; Verlag GmbH & Co.: Weinheim, 2004.
(8) Treat, N. D.; Ayres, N.; Boyes, S. G.; Brittain, W. J. *Macromolecules* **2006**, *39*, 26–29.
(9) Ayres, N.; Cyrus, C. D.; Brittain, W. J. *Langmuir* **2007**, *23*, 3744–3749.
(10) Ayres, N.; Boyes, S. G.; Brittain, W. J. *Langmuir* **2007**, *23*, 182–189.
(11) Pirri, G.; Chiari, M.; Damin, F.; Meo, A. *Anal. Chem.* **2006**, *78*, 3118–3124.
(12) Perrier, S.; Takolpuckdee, P.; Mars, C. A. *Macromolecules* **2005**, *38*, 6770–6774.
(13) Li, C.; Benicewicz, B. C. *Macromolecules* **2005**, *38*, 5929–5936.
(14) Raula, J.; Shan, J.; Nuopponen, M.; Niskanen, A.; Jiang, H.; Kauppinen, E. I.; Tenhu, H. *Langmuir* **2003**, *19*, 3499–3504.
(15) Tsujii, Y.; Ejaz, M.; Sato, K.; Goto, A.; Fukuda, T. *Macromolecules* **2001**, *34*, 8872–8878.
(16) Zhao, Y.; Perrier, S. *Macromolecules* **2006**, *39*, 8603–8608.
(17) Xu, G.; Wu, W.-T.; Wang, Y.; Pang, W.; Zhu, Q.; Wang, P.; You, Y. *Polymer* **2006**, *47*, 5909–5918.
(18) Israels, R.; Gersappe, D.; Fasolka, M.; Roberts, V. A.; Balazs, A. C. *Macromolecules* **1994**, *27*, 6679–6682.
(19) Lupitskyy, R.; Roiter, Y.; Tsitsilianis, C.; Minko, S. *Langmuir* **2005**, *21*, 8591–8593.
(20) Zhou, F.; Zheng, Z.; Yu, B.; Liu, W.; Huck, W. T. S. *J. Am. Chem. Soc.* **2006**, *128*, 16253–16258.
(21) Zhao, B.; Brittain, W. J.; Zhou, W.; Cheng, S. Z. D. *Macromolecules* **2000**, *33*, 8821–8827.
(22) Xu, F. J.; Zhong, S. P.; Yung, L. Y. L.; Kang, E. T.; Neoh, K. G. *Biomacromolecules* **2004**, *5*, 2392–2403.
(23) Kaholek, M.; Lee, W.-K.; Ahn, S.-J.; Ma, H.; Caster, K. C.; LaMattina, B.; Zauscher, S. *Chem. Mater.* **2004**, *16*, 3688–3696.
(24) Zhao, B.; Brittain, W. J. *Macromolecules* **2000**, *33*, 8813–8820.
(25) Hathaway, B. J.; Holah, D. G.; Postlewaile, J. D. *J. Chem. Soc., Part 3* **1961**, 3215.
(26) Matyjaszewski, K.; Miller, P. J.; Shukla, N.; Immaraporn, B.; Gelman, A.; Luokala, B. B.; Siclovan, T. M.; Kickelbick, G.; Vallant, T.; Hoffmann, H.; Pakula, T. *Macromolecules* **1999**, *32*, 8716–8724.
(27) Mitsukami, Y.; Donovan, M. S.; Lowe, A. B.; McCormick, C. L. *Macromolecules* **2001**, *34*, 2248–2256.
(28) Lai, J. T.; Filla, D.; Shea, R. *Macromolecules* **2002**, *35*, 6754–6756.
(29) Michielsen, S. *Polymer Handbook*, 4th ed.; John Wiley & Sons: New York, 1999.
(30) Danis, P. O.; Karr, D. E.; Mayer, F.; Holle, A.; Watson, C. H. *Org. Mass Spectrom.* **1992**, *27*, 843–846.
(31) Advincula, R.; Zhou, Q.; Park, M.; Wang, S.; Mays, J.; Sakellariou, G.; Pispas, S.; Hadjichristidis, N. *Langmuir* **2002**, *18*, 8672–8684.
(32) Fadeev, A. Y.; McCarthy, T. J. *Langmuir* **2000**, *16*, 7268–7274.
(33) Husseman, M.; Malmstrom, E. E.; McNamara, M.; Mate, M.; Mecerreyes, D.; Benoit, D. G.; Hedrick, J. L.; Mansky, P.; Huang, E.; Russell, T. P.; Hawker, C. J. *Macromolecules* **1999**, *32*, 1424–1431.
(34) Boyes, S. G.; Brittain, W. J.; Weng, X.; Cheng, S. Z. D. *Macromolecules* **2002**, *35*, 4960–4967.
(35) Plunkett, K. N.; Zhu, X.; Moore, J. S.; Leckband, D. E. *Langmuir* **2006**, *22*, 4259–4266.
(36) He, Q.; Kuller, A.; Grunze, M.; Li, J. *Langmuir* **2007**, *23*, 3981–3987.
(37) Jakubowski, W.; Matyjaszewski, K. *Macromolecules* **2005**, *38*, 4139–4146.
(38) Min, K.; Gao,; Matyjaszewski, K. *Macromolecules* **2007**, *40*, 1789–1791.
(39) Matyjaszewski, K.; Dong, H.; Jakubowski, W.; Pietrasik, J.; Kusumo, A. *Langmuir* **2007**, *23*, 4528–4531.

MA800154C